Combined distributed temperature sensing and current monitoring

Sebastian G.M. Krämer[ab], Wilhelm Feichter[b], Fernando Puente León[a], Jörg Stromberger[b]
[a]TU München, Fachgebiet Verteilte Messsysteme, Theresienstr. 90/N5, 80333 Munich, Germany
[b]GE Global Research, Hybrid & Renewables Energy Systems Lab, Garching, Germany

ABSTRACT

Power cables should be operated at an adequate temperature level. Therefore, numerous power utilities have installed optical distributed temperature sensing (DTS) systems to measure the temperature of underground cables. Protection and metering systems used in power systems require measurements of the current flowing in the high-power conductors as well. Optical current sensors achieve increasing attention and acceptance for this application due to their inherent electrical insulation, high bandwidth, and immunity to EMI. DTS systems are based on spontaneous Raman scattering or Brillouin scattering, which use spectral information in the reflected light, whereas optical current sensors are based on the Faraday effect, which changes the intensity of transmitted light. This paper proposes a novel design of a combined optical temperature and current measurement system, using both physical effects. A first measurement setup is described, and first results are discussed. Thereby, the specifications for the combined data acquisition and data processing unit are analyzed in order to optimize the accuracy and the reliability of each subsystem and the whole system.

Keywords: fiber-optic sensors, distributed temperature sensing, Faraday effect, Raman effect

1. INTRODUCTION

High-voltage cable lines for electrical power transmission are widespread and used for different applications. Especially new fields of application, like connecting off-shore wind farms and sub-sea power distribution systems, make great demands on these cable systems. Cross-linked polyethylene (XLPE) and high pressure fluid-filled (HPFF) cables have been used extensively in underground transmission circuits at 220 kV and above in Europe, the Middle East and Asia. The insulation system of a HPFF cable includes pressurized oil that circulates inside the steel pipe conduits of the power cables. In the case of failures in the oil handling and processing equipment or due to a leak in a steel pipe conduit (e.g., due to corrosion or excavation near the cable trench), substantial amounts of oil may inadvertently be released to the environment. The insulation system in an XLPE cable, on the other hand, is based on a solid dielectric and, therefore, there is no risk of oil release for the environment.

Breakdowns of these lines often cause extensive consequential damage of the whole system. Further the special and harsh environment makes it necessary to have a remote condition and fault analysis system. Traditionally, two measurement type groups are applied, offline and online. Offline methods are based on electro-chemical (dissolved gas analysis) and dielectric (partial discharge measurement, dielectric spectroscopy, and isothermal relaxation current) effects [1]. Usually, the cable line has to be shut down or needs to be removed for this type of test. This is cost-intensive and in some cases even impossible.

State-of-the-art methods for online measurements in sub-sea cables are distributed temperature sensing and current measurement, in addition to water penetration monitoring. Protection and metering systems used in power systems require measurements of the current flowing in the high power conductors as well. Usually, traditional current transducers, based on inductive current transformers, and Hall effect sensors are used for high-current measurements on high-voltage lines. Current transformers are designed to provide a current in its secondary winding which is proportional to the current flowing in the primary one. They are commonly used in metering and protective relaying in the electrical industry, where they facilitate a safe measurement of large currents, as they isolate the measurement circuit from the high voltage source. However, the accuracy and frequency range of current transformers is related directly to a number of factors like rating factor, external electromagnetic field, temperature, and physical configuration.

Fiber Optic Sensors and Applications V, edited by Eric Udd, Proc. of SPIE
Vol. 6770, 677015, (2007) · 0277-786X/07/$18 · doi: 10.1117/12.734091

2. FIBER-OPTIC CURRENT SENSING

Fiber-optic sensors are robust with respect to EMI, as the physical parameters are directly converted into an optical signal in an optical device such as an optical fiber or an optical crystal. Hence, the electrical signal noise is not transmitted to the data acquisition unit. Another advantage of fiber-optic current sensors (FOCS), apart from the reduced weight, is the fact that the sensor cannot be damaged by over current coming from an unexpected surge.

2.1 Fiber-Optic Current Sensing

The Faraday effect, used for electrical current and magnetic field measurements, is a magnetically induced circular birefringence. For diamagnetic and paramagnetic materials, a linearly polarized light travelling in the direction of a magnetic field experiences a net rotation Θ, such that

$$\Theta(\lambda, T) = V(\lambda, T)\int H\, dl \,, \tag{1}$$

where Θ denotes the measured angle of rotation of the field, λ the free-space wavelength of light, T the ambient temperature, V the Verdet's constant of the magneto-optic material, and H the magnetic field intensity along the propagation path l. The Faraday effect is illustrated in Fig. 1.

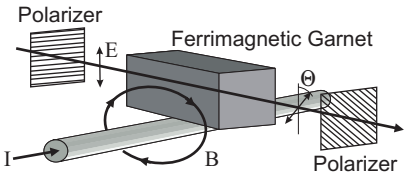

Fig. 1 Principle of Faraday rotation.

Depending on the applied optical materials, two different configurations based on the Faraday effect are commercially available. One solution works with an optical fiber wounded N times around the conductor. The angle Θ, through which the polarization plane of light rotates in the fiber in the presence of a magnetic field induced by the current I in the wire, is given by [2]:

$$\Theta = VNI \,, \tag{2}$$

where V denotes the Verdet's constant of the magneto-optic material. To achieve a high signal-to-noise ratio in the output signal, several turns N of the sensing fiber around the current carrying wire are needed, and different optical paths and light rotation detection methods have been developed to eliminate external effects.

Another configuration, which has been used for our experiments, works with optically transparent ferri- and ferromagnetic crystalline materials featuring a large Verdet constant and hence a bigger sensitivity due to an increased rotation angle per length l. Ferrimagnetic iron garnet crystals exhibit a magneto-optic sensitivity that is orders of magnitude higher than those of typical paramagnetic and diamagnetic materials. Substitute garnets, such as Ga:YIG, exhibit larger sensitivities, though often with lower resonance frequencies that decrease the bandwidth [3].

2.2 FOCS Measurement Setup

For low frequencies, the magnetic near field induced by an electrical current can be calculated by the Biot-Savart law:

$$d\vec{H} = \frac{Id\vec{l} \times \vec{r}}{4\pi r^3}, \tag{3}$$

where H denotes the magnetic field, I the current in a given wire segment, dl the length element of the wire, and r the displacement vector from the element to the field point.

To measure electric currents, the sensing element of the fiber-optic magnetic field sensor has to be placed as close as possible to the cable to detect the magnetic field produced by the current and to minimize effects resulting from sources of interference. In the sensor head, the magneto-optic iron garnet is arranged between two polarizers (Fig. 1). As a light source, a superluminescent diode (SLD) is used, which couples the light into an optical fiber feeding the sensor head.

The output of the sensor head is an intensity-modulated light signal which is transported to an opto-electrical (o/e) converter via another optical fiber.

Ferrimagnetic iron garnet crystals feature a bandwidth of over 500 MHz [3]. Substituted garnets, such as Ga:YIG, exhibit larger sensitivities, but often with lower resonance frequencies which decrease the bandwidth. In any case, such specifications are even suitable for high-frequency current measurements. Thus, the limiting factors are the amplifiers in the o/e converter and the sample rate of data acquisition units. To simulate high currents during our presented experiments, the sensor was put into a coil.

2.3 Distributed Temperature Sensing

Distributed fiber-optic temperature sensors make it possible to monitor the temperature profile along the length of a fiber continuously. Distributed temperature sensing (DTS) based on optical fibers was first demonstrated in 1981 at Southampton University while using techniques derived from telecommunications cable testing. The original work used special fibers which resulted in limited temperature range and distance coverage, but good response time and spatial resolution [4]. Further research on Raman scattering in fibers has provided a technology to cover much longer distances and a wider temperature range using standard single-mode and multi-mode fibers [5–7].

The sensors operate with the powerful optical time domain reflectometry (OTDR) principle, invented by Barnowski and Jensen in 1976, which was the first method for distributed fiber measurements using backward Rayleigh scattering to determine the optical loss along fibers [8]. A short laser pulse is sent along the fiber, and the backscattered Raman light is detected with high temporal resolution. The intensity of the Raman light contains information about both loss and temperature along the fiber, whereas the time between sending the pulse and detecting the backscattered signal provides a measure of the distance along the fiber. As the DTS system is based on optical fiber technology, it can be used in a wide range of conditions, including hazardous environment and EMI intensive areas, such as power cable monitoring, fire detection in tunnels, and pipeline monitoring.

2.4 Raman Light Scattering

Light is scattered as the pulse passes down the fiber through several mechanisms, including density and composition fluctuation (Rayleigh scattering) as well as Raman and Brillouin scattering due to molecular and bulk vibrations, respectively (Fig. 2). The effects of scattering are classified by the relation between the frequencies of the incident and those of the scattered photons. When these frequencies or wavelengths are equal, it is called *unshifted*, *Rayleigh* or *elastic* scattering. But if these frequencies differ, the terms *shifted* or *inelastic* scattering are used. Examples are the Raman and Brillouin scattering, which are both temperature sensitive. In practice, the Brillouin lines are separated

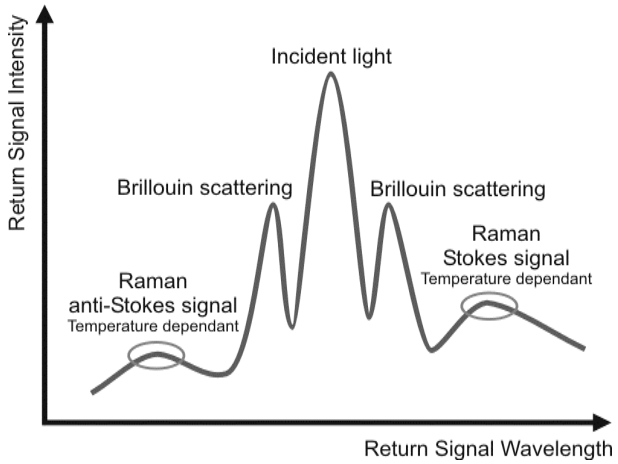

Fig. 2 Spectrum of backscattered light.

from the launch wavelength by only a few tens of GHz, and it is impractical to separate these components from the Rayleigh signal. The Raman signal, however, is sufficiently strong and distinct to be useful in temperature measurement. Here the frequency shifts equally to the characteristic vibrational frequencies of the molecules. Photons scattered to lower frequencies are termed Stokes lines, and those scattered to higher frequencies are termed the anti-Stokes lines. The longer wavelength Stokes line is only weakly temperature-sensitive, whereas the backscattered light at the shorter anti-Stokes wavelength increases with an increase in temperature.

3. PROPOSED APPROACH

The use of spontaneous Raman scattering in optical fibers is of current interest in sensor applications [5]. This effect can be used to measure distributed temperature along a sensor fiber. For the locally distributed measurement of the Raman scattered light, an optical backscatter process is required. The best known back scatter process is the OTDR (optical time-domain reflectrometry). This process needs a high-performance pulsed laser source for temperature measurements in the backscattered light. The second process is the OFDR (optical frequency-domain reflectrometry). Optical distributed temperature sensing systems (DTS) are based on both methods [6].

FOCS are based on the Faraday effect, which is a type of magneto-optic effect [7]. When polarized light propagates across an optical medium (fiber or crystal) and the direction of propagation of the light wave is parallel to the direction of propagation of the induced magnetic field wave, the Faraday effect induces a rotation of the plane of polarization of the optical wave. Polarizers in front of and after the magneto-optic material transform this rotation into a change of intensity of light. By aligning an optical fiber along a high-voltage power cable, the magnetic field along the cable and the electric current can be derived.

FOCS use the information in the transmitted part of light in an optical fiber, whereas DTS gain their information from the reflected part. Both physical effects have no direct interference. This paper describes a combination of both sensor systems. The physical and technical aspects of a combined optical sensor system are evaluated with the proposed measurement setup depicted in Fig. 3.

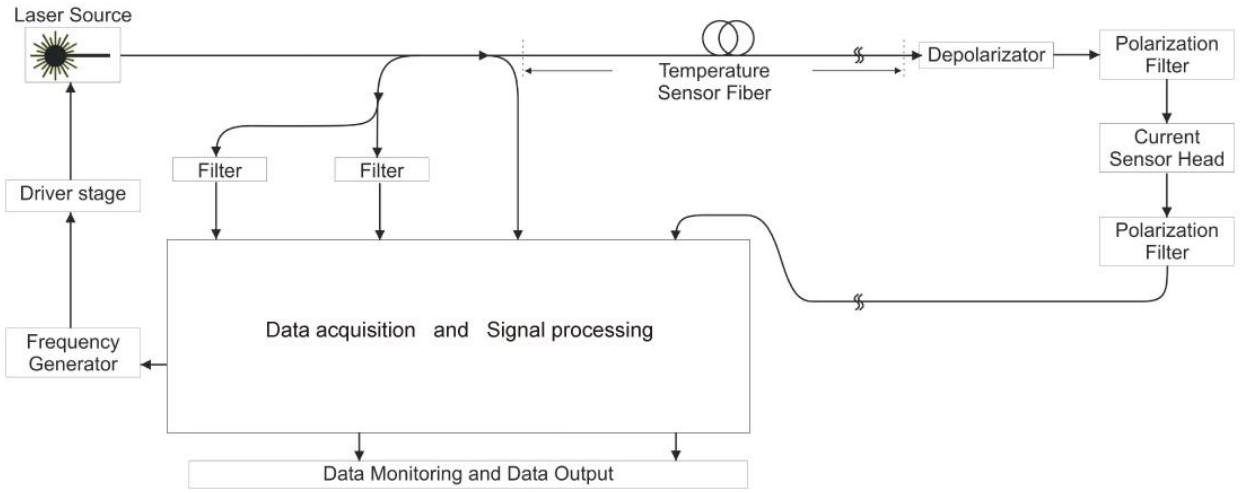

Fig. 3 Scheme of a combined optical current and temperature measurement system.

Light of a pulsed light source passes first through the temperature-sensitive fiber segment. Hot spots cause reflective light emissions according to the Raman effect. These reflective parts of the light are filtered for the Stokes/anti-Stokes line detection. The position and temperature value of hot spots are derived in a signal processor unit, and the results are transmitted to a data monitoring system. The remaining unreflected light is transmitted through the fiber and sustains a rotational shift according to the Faraday effect. To measure the rotational shift, the FOCS requires a reference source, which is obtained from the DTS system. A data processing system calculates the applied magnetic field along the fiber and the electric current in the attached power line.

The data monitoring system combines thermal and electrical measurements and shows the condition of the monitored power line according to its power rating.

4. EXPERIMENTAL RESULTS AND DISCUSSION

To investigate the coexistent effect of Raman scattering and Faraday effect, a sophisticated laboratory setup was developed and built up. The experimental setup consists of several parts depicted in Fig. 4.

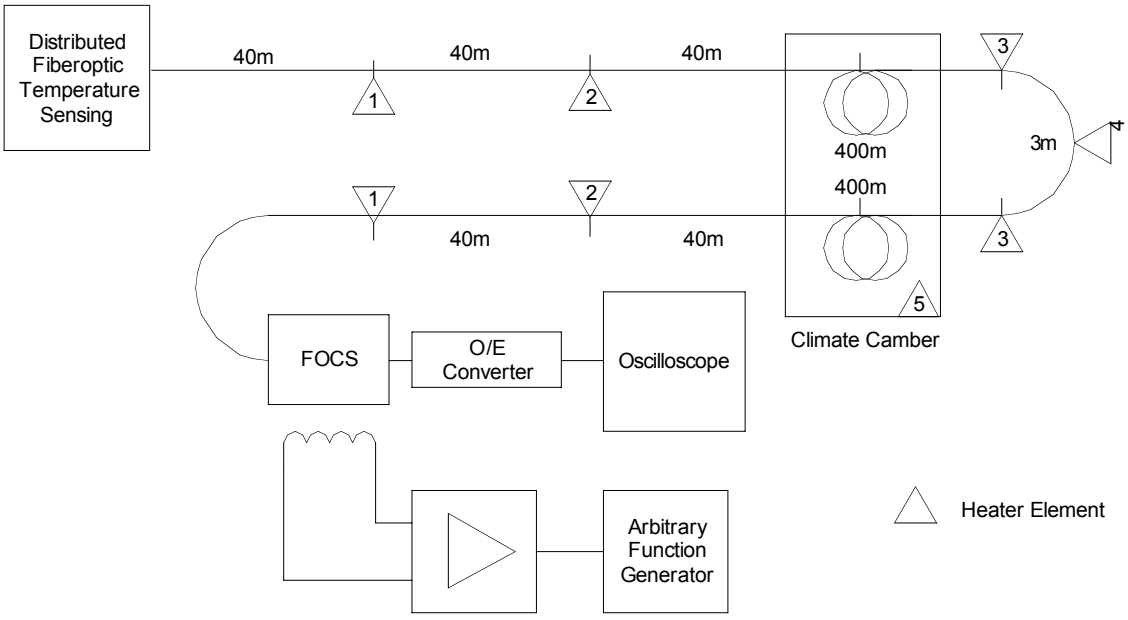

Fig. 4 Experimental setup.

As a distributed sensing element, a standard 1020 m (0.63 mile) 0.27 NA Graded Index multi-mode fiber was used. Four individually controllable groups of electrical heating elements were attached to the fiber in order to simulate hot spots. Two hot spots were applied at the first 120 m and the last 80 m of the fiber. Each heating element had a total maximum power of at least 10 watts. Furthermore, two loops of approximately 400 m were placed inside a climate chamber that is able to cool down to –40 °C / –40 °F. Between these two loops, a 3 m fiber part was lead out of the chamber and attached with three further heating elements.

For the distributed temperature measurement, a commercial system was utilized. The DTS uses a proprietary code correlation technique related to a Golay code. This coding allows using class 1M lasers. The DTS is capable to measure temperature differences of 0.65 K at a 1.5 m spatial resolution on up to 8 km long fibers in a 10 min measurement interval. The system has a wide measurement range from –250 °C to 400 °C.

All measurements were taken with a spatial resolution of 1.5 m and a measurement time of 1 min. To simulate the current behavior of a power line, a coil was attached to the FOCS. An arbitrary function generator controls an amplifier, which drives a sine wave voltage. The intensity measurement of the transmitted laser light was done by an optical-electrical converter and displayed with an oscilloscope.

First measurements were done by testing the temperature sensing capabilities for hot spots.

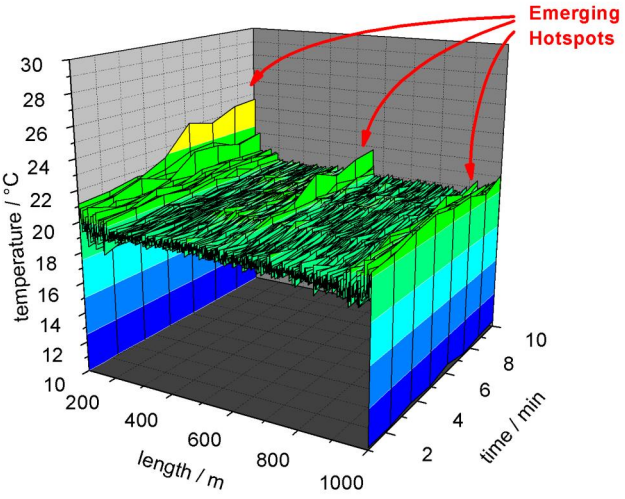

Fig. 5 DTS Temperature measurement over 10 minutes.

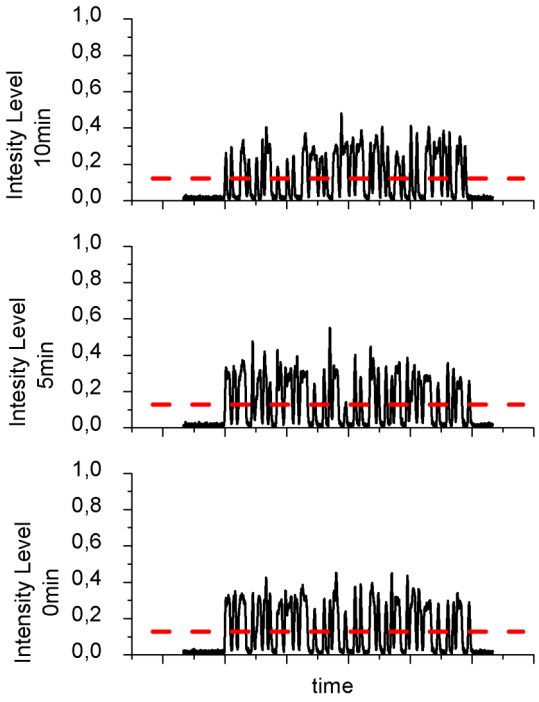

Fig. 6 FOCS measurements over 10 minutes.

All four hot-spot elements were switched on after 5 minutes. While the climate chamber held the middle segments on a constant temperature of 19 °C, the first and last 120 m of the fiber were exposed to an increased ambient temperature of 22+ °C (Fig. 5). Intensity measurements of the light transmitted through the FOCS, which were taken simultaneously, showed no interference (Fig. 6), and the calculated mean values of the transmitted light intensity remained at a constant level.

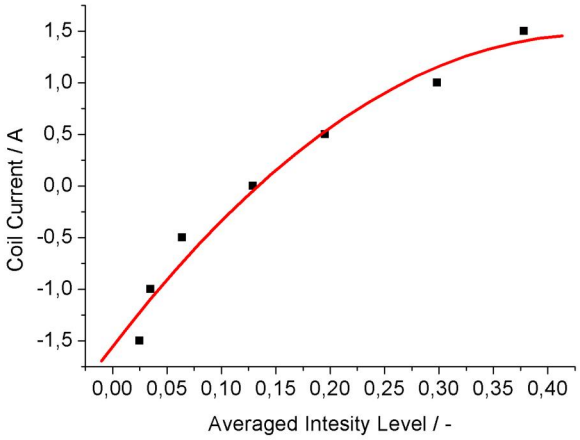

Fig. 7 Current vs. light transmission intensity.

The next experiments showed the intensity response caused by the Faraday effect, with an applied DC coil current of 0.5 A to 1.5 A (Fig. 8). The heating elements stayed at a constant level, and simultaneously taken readings from the DTS system showed no effect (Fig. 9). Possible effects, like reflections at the end of the fiber, caused by the FOCS crystal surface, could not be observed with the proposed measurement setup.

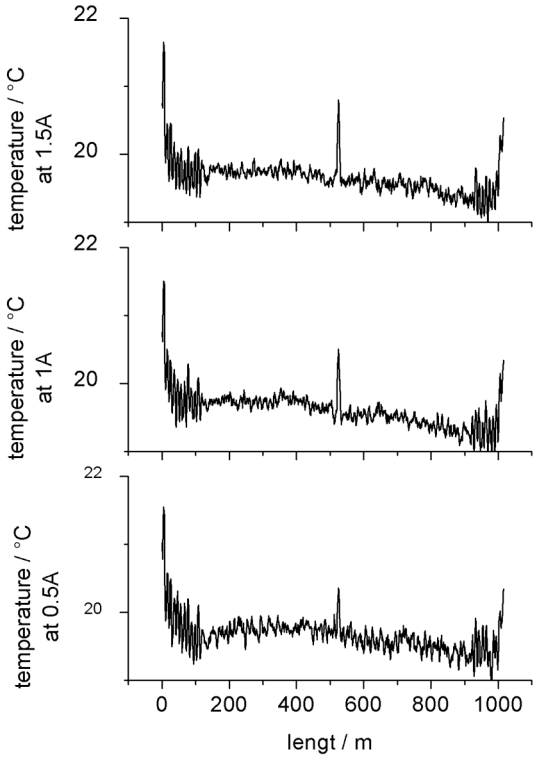

Fig. 8 DTS measurements with different FOCS current levels.

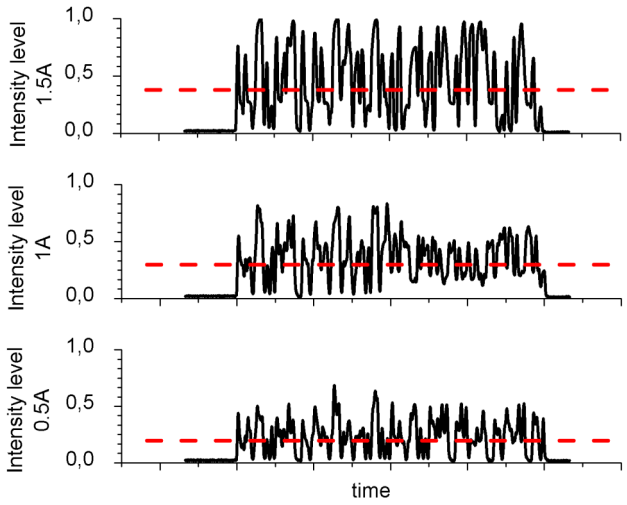

Fig. 9 Averaged FOCS intensity at different current levels.

The averaged intensity measurement displayed to be a simple mathematic current coherence (Fig. 7).

$$I_{FOCS} = -1.5 + 13.7 \cdot V_{Optical} - 15.5 \cdot V_{Optical}^2 \quad (4)$$

The last measurement shows a typical power-line fail in subsea cables–an escalating hot spot. To have an adequate statement of hot spots, simultaneous measurements of the distributed line temperature and current levels have to be done. In this case, the climate chamber kept the fiber at a constant level of 4°C. The 3 m in the middle of the line were lead out of the chamber and possessed the ambient temperature (22°C); this was considered in the hot spot recognition. First, the current was increased slowly. After 10 minutes, hot spot number 4 was activated to simulate an insulation break. Measurements taken from the DTS and the FOCS system were evaluated online and linked to detect a line fault.

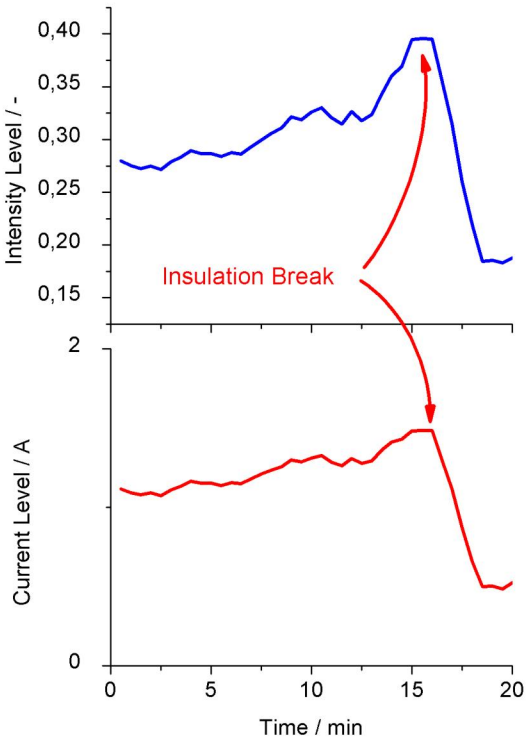

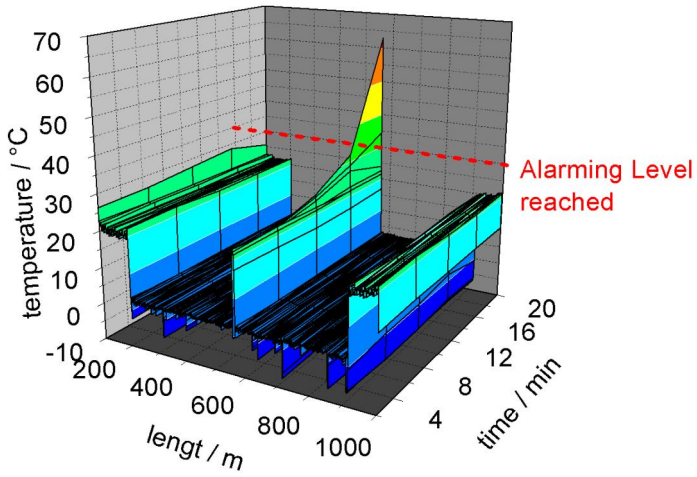

Fig. 11 DTS measurements with an emerging hot spot.

Fig. 10 Transmitted light and current levels.

The DTS system recognizes emerging hot spots and is able to signal them to a control system (Fig. 11). After the insulation of the power cable was breaking down, typically a short-circuit current detection reacts and switches off the power line (Fig. 10). With the combination of the optical current measurement of the FOCS, this system is able to compute a trend and could react in the case of a potential line fault.

5. CONCLUSION

The successful combination of two different optical measurement principles in one optical fiber was shown by the presented experiments. It could be assumed that reflections at the FOCS crystal surfaces interfere with the DTS measurement system by causing attenuation at the end of the fiber, but our measurements let assume that this is not the case. The used DTS system was capable of reliable hot spot detection. Precision and speed are sufficient enough for an industry-grade application. For some applications, a measurement range higher than 8 km could be helpful. The FOCS has shown that it could be a good replacement for the traditional current transducers. The system is relatively robust against environmental influences, if a proper packaging is considered. Optical temperature measurement in cable systems is state-of-the-art. The optical systems for current measurement are a growing field for optical sensing systems. Combing both optical measurement methods to one reliable, compact-sized system, could be helpful in various remote power cable applications, where outage times are mission-critical.

ACKNOWLEDGEMENT

The authors gratefully acknowledge financial support of this work by GE Global Research Europe and the Karl-Max von Bauernfeind Association.

REFERENCES

1. G. Hoff and H.-G. Kranz, "Isothermal relaxation current analysis: A new non-destructive diagnostic tool for polymeric power distribution cables," IEEE / PES Panel on Diagnostic Measurement Techniques for Power Cables, 1999.
2. K. Bohnert et al., "Temperature and vibration insensitive fiber-optic current sensor," Journal of Lightwave Technology 20, 267–276, 2002.
3. K.B. Rochford et al., "Improved fiber-optic magnetometer based on iron garnet crystals," 14th Optical Fiber Sensors Conference, pp. 332 – 335, 2000.
4. York Sensors Ltd., "Technical aspects of optical fibre distributed temperature sensing," IEE Colloquium on Operational Monitoring of Distribution and Transmission Systems (Digest No. 1997/050), pp. 3/3 – 3/7, 1997.
5. J.P. Dakin, D.J. Pratt, G.W. Bibby, and J.N. Ross, "Distributed optical fibre Raman temperature sensor using a semiconductor light source detector," Electron. Letter, 569 – 570, vol. 21, 1985.
6. A.H. Hartog, A.P. Leach, and M.P. Gold, "Distributed temperature sensing in solid-core fibres", Electron. Letter, vol. 21, 1061–1062, 1985.
7. T. Wakami and S. Tanaka, "1.55 μm long span fibre optic distributed temperature sensor," Int. Conf. Optical Fibre Sensors OFS94, pp. 134 – 137, 1994
8. M.K. Barnowski and S.M. Jensen, "Fiber waveguides: A novel technique for investigating attenuation characteristics," Appl. Opt., vol. 15, 2112–2115, 1976.